

Quadrupole collective modes in trapped finite-temperature Bose-Einstein condensates

B. Jackson and E. Zaremba

Department of Physics, Queen's University, Kingston, Ontario K7L 3N6, Canada.

(March 22, 2002)

Finite temperature simulations are used to study quadrupole excitations of a trapped Bose-Einstein condensate. We focus specifically on the $m = 0$ mode, where a long-standing theoretical problem has been to account for an anomalous variation of the mode frequency with temperature. We explain this behavior in terms of the excitation of two separate modes, corresponding to coupled motion of the condensate and thermal cloud. The relative amplitudes of the modes depends sensitively on the temperature and on the frequency of the harmonic drive used to excite them. Good agreement with experiment is found for appropriate drive frequencies.

PACS numbers: 03.75.Fi, 05.30.Jp, 67.40.Db

One of the most significant challenges facing theorists studying Bose-Einstein condensation (BEC) is to understand the finite-temperature properties of trapped gases, where the noncondensed fraction is significant. For instance, while solutions of the Gross-Pitaevskii (GP) equation for low-lying collective modes [1] yield good agreement with experiments at low temperatures [2], the behavior at elevated temperatures is still not fully understood. The quadrupole modes studied in an early experiment by Jin *et al.* [3] have been especially problematic. In this experiment, a harmonic modulation of the trap frequency was used to selectively excite either $m = 0$ or $m = 2$ modes, and the frequency and damping of the modes as a function of temperature, T , were extracted from the subsequent response. Although several theories have been proposed that account for the observed damping [4,5] and frequency of the $m = 2$ mode [5–7], the experimental data for the $m = 0$ frequency has yet to find a satisfactory explanation.

The difficulty is apparently related to the fact that the frequency of the $m = 0$ condensate mode lies relatively close to that of the corresponding noncondensate mode. In particular, the condensate frequency at $T = 0$ in the Thomas-Fermi (high density) limit is $\omega = 1.80\omega_{\perp}$ [1] (where ω_{\perp} is the axial trap frequency), while the thermal cloud has a natural frequency of oscillation at $\omega = 2\omega_{\perp}$. It should be emphasized that the latter is not a true collective mode but is rather a coherent motion of the atoms in a harmonic potential. At temperatures below T_c , where the condensate coexists with a significant thermal fraction, these two modes of oscillation are strongly coupled by mean-field interactions. As a result, a harmonic drive will tend to excite a superposition of the two, and the observed $m = 0$ condensate frequency will reveal this coupling. A consistent theoretical model

should therefore include the full dynamics of the thermal cloud, and treatments that neglect fluctuations of the noncondensate [6] or include them perturbatively [5,8,9] will not capture this behavior.

To avoid this shortcoming, Refs. [10,11] used a variational scheme to solve coupled GP and Boltzmann kinetic equations to describe the dynamics of, respectively, the condensate order parameter and the noncondensed component. Normal modes corresponding to in-phase and out-of-phase oscillations of the two components were found, and the authors suggested that the $m = 0$ experimental data could be explained as a cross-over between the two modes. As we shall see, this picture in fact has some validity, however a quantitative interpretation of the experiments requires a more accurate treatment of the thermal cloud. In particular, Landau damping, which is the dominant damping mechanism in this regime, was not included since the variational ansatz used precludes coupling to higher order modes. Moreover, in view of our earlier comment about the nature of the thermal cloud oscillation, it is unclear to what extent the simple normal mode picture for the thermal cloud is meaningful.

In this work we model the experiment of Jin *et al.* [3] using numerical simulations based upon the ZNG formalism [12]. This approach was previously applied to the scissors mode [13] and yielded good agreement with experiment [14]. We evolve a GP equation simultaneously with a semiclassical kinetic equation, where the latter is solved by representing the thermal cloud by means of an ensemble of test particles which suffer collisions with each other as well as with the condensate. Importantly, since the particles are also coupled to the condensate through mean-field interactions, our model includes Landau damping (and corresponding frequency shifts) of condensate oscillations. Further details of the numerical method can be found in [15].

By using different initial conditions we can separately excite motion of the condensate and thermal cloud. Alternatively, by imposing a harmonic modulation of the trap frequencies over a finite interval (in a similar fashion to experiment), we excite both components simultaneously. At high temperatures we find that the condensate exhibits oscillations with two frequency components — one corresponding to a damped oscillation of the condensate interacting with a quasistatic bath of thermal particles, and a second arising from the mechanical coupling to the oscillation of the thermal cloud. The relative amplitudes of the two components depends on temperature and on the frequency of the harmonic drive. By using different drives we can closely reproduce the ob-

served temperature dependence of the $m = 0$ frequency.

The GP equation for the condensate wavefunction, $\Phi(\mathbf{r}, t)$, and the Boltzmann kinetic equation for the thermal cloud phase space density, $f(\mathbf{p}, \mathbf{r}, t)$, are respectively given by

$$i\hbar \frac{\partial \Phi}{\partial t} = \left(-\frac{\hbar^2 \nabla^2}{2m} + U_{\text{eff}} - gn_c - iR \right) \Phi, \quad (1)$$

$$\frac{\partial f}{\partial t} + \frac{\mathbf{p}}{m} \cdot \nabla f - \nabla U_{\text{eff}} \cdot \nabla_{\mathbf{p}} f = C_{12}[f] + C_{22}[f]. \quad (2)$$

The above equations are derived under certain approximations [12]. Importantly, thermal excitations are treated within the Hartree-Fock (HF) and semiclassical approximations [16], where they can be identified with particles moving in an effective potential $U_{\text{eff}} = m\omega_{\perp}^2(x^2 + y^2 + \lambda^2 z^2)/2 + 2g(n_c + \tilde{n})$. Here, $n_c(\mathbf{r}, t) = |\Phi(\mathbf{r}, t)|^2$ and $\tilde{n}(\mathbf{r}, t) = \int (d\mathbf{p}/h^3) f(\mathbf{p}, \mathbf{r}, t)$ are the condensate and noncondensate densities respectively ($g = 4\pi\hbar^2 a/m$, where a is the s-wave scattering length and m is the atomic mass). The integral C_{12} represents collisions that transfer atoms between the condensate and noncondensate, while C_{22} collisions take place between thermal particles only. The former process couples to the GP equation through $R(\mathbf{r}, t) = (\hbar/2n_c) \int (d\mathbf{p}/h^3) C_{12}[f]$ and leads to a change in the number of condensate atoms.

Our simulation parameters are chosen to match those of the experiment [3], where $\omega_{\perp} = 2\pi \times 129 \text{ Hz}$ and $\lambda = \sqrt{8}$. The equilibrium densities of the condensate and noncondensate are found using a self-consistent semiclassical procedure [12,17] at each temperature. Due to evaporative cooling the total number of atoms, N , in the experiment varied with temperature. This is accounted for in our simulations by using experimental data for the temperature and number of *condensate* atoms, the variables believed to be the most precisely determined [18]. Alternatively, we have also used the temperature and *total* number of atoms to specify the state of the system. Although this leads to slightly different equilibrium conditions, it does not affect the general conclusions of our work. These experimental uncertainties, however, should be kept in mind when making comparisons between theory and experiment.

We can excite quadrupole modes by imposing velocity fields of the form $\mathbf{v}_c = A_{c0}(x, y) + A_{c2}(x, -y)$ onto the condensate, and $\mathbf{v}_n = A_{n0}(x, y) + A_{n2}(x, -y)$ onto the noncondensate. In the case of the condensate, the velocity is established by multiplying the equilibrium condensate wavefunction by an appropriate phase factor. For the thermal cloud, we simply add the position-dependent \mathbf{v}_n to the initial velocity of each test particle. Since the $m = 0$ and $m = 2$ modes are decoupled from each other due to their different symmetries, it is advantageous to excite both simultaneously (e.g., $A_{c0}, A_{c2} > 0$). The corresponding modes are then projected out in the ensuing evolution by evaluating the moments $Q_{\{n,c\}0} = \langle x^2 + y^2 \rangle_{\{n,c\}}$ ($m = 0$) and $Q_{\{n,c\}2} = \langle x^2 - y^2 \rangle_{\{n,c\}}$

($m = 2$). We note that the ($l = 0, m = 0$) monopole and ($l = 2, m = 0$) quadrupole modes of an isotropic trap are coupled by the trap anisotropy [1], giving rise to low and high frequency $m = 0$ modes. Only the low-lying $m = 0$ out-of-phase breathing mode is appreciably excited by the initial conditions considered here.

For our first simulations, we excite oscillations in the condensate alone (i.e., $A_{n0} = A_{n2} = 0$). The Q_n amplitudes remain small during the course of the evolution, while the condensate oscillations are damped. To extract frequencies and damping rates we fit a single exponentially-decaying sinusoid to the data over the timescale of the simulation, $\omega_{\perp} t = 25$. The open squares in Fig. 1 show the frequencies as a function of the reduced temperature $T' = T/T_c^0$, where $T_c^0 = 0.94\hbar\omega_{\perp}(\lambda N)^{1/3}/k_B$ is the ideal gas critical temperature. Apart from the highest temperature at $T' = 0.9$, the single function fit is very good, consistent with an excitation of just one mode of each symmetry. For both the $m = 0$ and $m = 2$ modes we find a marked downward frequency shift with increasing temperature, in agreement with previous theories that neglect the full noncondensate dynamics [5–7], and with the out-of-phase “condensate” mode in Ref. [10]. Also, as in earlier treatments, we find that there is much better agreement with the experimental $m = 2$ data than with the $m = 0$ data above $T' = 0.6$.

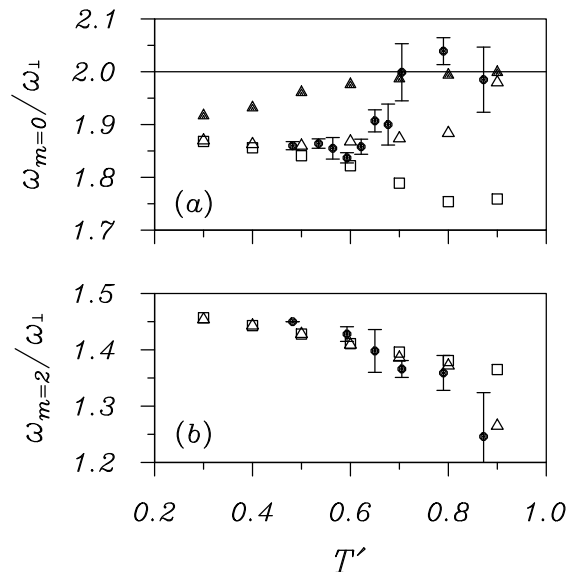


FIG. 1. Frequencies of the (a) $m = 0$ and (b) $m = 2$ modes as a function of reduced temperature $T' = T/T_c^0$. Data from the experiment of Ref. [3] is plotted with error bars, while our frequency results are shown for the condensate (open symbols) and noncondensate (filled symbols). Different initial conditions are represented by squares ($A_{n0}, A_{n2} = 0$) and triangles ($A_{n0}, A_{n2} > 0$), where for both $A_{c0}, A_{c2} > 0$.

We next investigate the influence of the thermal cloud

dynamics by exciting both components simultaneously. In these simulations, the velocity fields imposed on the condensate and thermal cloud are identical. The triangles in Fig. 1 show results of a single mode fit to the condensate and noncondensate data. At high temperatures the thermal cloud oscillates with a frequency close to the ideal gas value, $\omega = 2\omega_{\perp}$, which decreases as the temperature is lowered. The $m = 2$ condensate frequency is largely independent of the initial condition (indeed it is also unchanged for a harmonic modulation of the trap discussed below), apart from the highest temperature point where the condensate mode becomes ill-defined. In contrast, the $m = 0$ condensate frequencies are generally higher than those found by exciting the condensate alone, and approach the noncondensate value just below the transition.

Further insight into this behavior can be gained by fitting two damped sinusoids to the $m = 0$ condensate data. This shows that two modes are present at high temperatures, with one frequency close to that found for the condensate-only excitation. The second matches the noncondensate value, and indicates that the condensate is being driven by the thermal cloud at its own natural frequency (through mean field interactions and C_{12} collisions). Following Ref. [10] we refer to these as the “condensate” and “thermal cloud” modes, respectively. The observed condensate oscillation is thus a superposition of the two modes, with the relative amplitudes being sensitive to the initial conditions. By using a single mode fit to analyze the data, a frequency intermediate between the two mode frequencies is obtained, as shown by the open triangles in Fig. 1(a). In the case of the $m = 2$ modes, the condensate and noncondensate frequencies are sufficiently separated for the noncondensate to have a minimal effect on the condensate, and the latter thus oscillates at a frequency which is independent of the method of excitation.

Qualitatively, the behavior of the $m = 0$ mode shown by the open triangles in Fig. 1(a) is reminiscent of that exhibited experimentally [3]. However, a quantitative comparison to experiment requires simulations which more faithfully reproduce the harmonic excitation scheme employed experimentally. In the simulations to be described next, the axial trap frequency is modulated according to $\omega_{\perp}^2(t) = \omega_{\perp}^2(1 + \epsilon \sin \Omega t)$ over a time interval of $\omega_{\perp}t = 30$, before allowing the sample to evolve in the original trap potential for another $\omega_{\perp}t = 30$. This excites $m = 0$ type oscillations in both the condensate and thermal cloud. Typical time-dependent plots of Q_{c0} and Q_{n0} are shown in Fig. 2 for $\Omega = 1.95$ and $T' = 0.8$. In the case of the condensate, we clearly see beating between the condensate and thermal cloud modes after removal of the excitation. This should be observable if experimental measurements are extended to longer times.

In the experiments, a single mode fit was used to extract mode frequencies from the data in a time interval of approximately $\omega_{\perp}t = 15$ following the excitation. We have followed this procedure by analyzing our data within

the observation window indicated by the vertical lines in Fig. 2. Very different results for the condensate frequency are obtained depending on the drive frequency Ω which affects the relative amplitude of the condensate and thermal cloud oscillations. Fig. 3 summarizes our results by showing frequencies from single-mode fits at each T for drive frequencies in the range $[1.75, 2.00] \omega_{\perp}$. At low T the noncondensed component is small and has a minimal effect. As a result, all the frequencies are close to the condensate mode results shown by the open squares in Fig. 1. In contrast, above $T' \sim 0.6$ there is a significant spread in the frequencies extracted from the fits. Taking $T' = 0.8$ as an example, the condensate mode is excited when $\Omega \simeq 1.75\omega_{\perp}$, while the frequency is close to that of the thermal cloud mode when $\Omega \simeq 2\omega_{\perp}$.

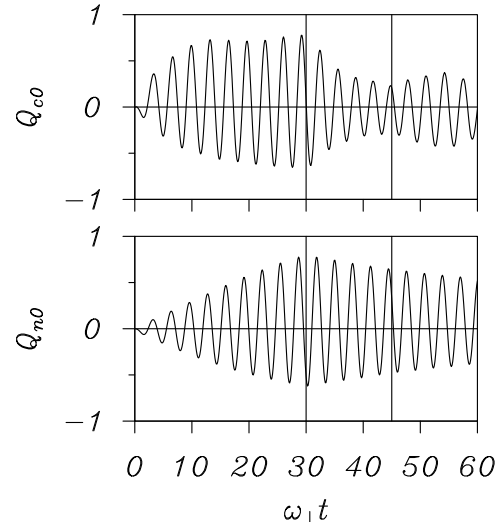


FIG. 2. Plot of the condensate and noncondensate $m = 0$ quadrupole moments Q_{c0} , Q_{n0} (in arbitrary units) as a function of time, at $T' = 0.8$. During the first $\omega_{\perp}t = 30$ (up to the first vertical line) the system is driven by a trap modulation of frequency $\Omega = 1.95\omega_{\perp}$ and amplitude $\epsilon = 0.02$. The subsequent evolution takes place in a static trap, where the second vertical line indicates the approximate range of experimental measurements.

It is clear from our data that there are two distinct branches above $T' \sim 0.7$. The lower branch follows closely the condensate mode in Fig. 1 while the upper branch moves up to the thermal cloud frequency. Although the precise drive frequency used in the experiments is no longer known [18], the frequency was chosen to maximize the amplitude of the condensate oscillation. Using this criterion, we have identified the drive frequencies that give a large response by the solid points in Fig. 3. Again there are two clear branches, and although experiment could feasibly have followed either, the upper branch clearly seems most relevant. Given the uncertainties in the experimental conditions the agreement is pleasing, and is strong evidence that a cross-over from one branch to the other is responsible for the observed

temperature dependence. Our simulations nevertheless indicate that the lower branch should be observable if driven at the appropriate frequency.

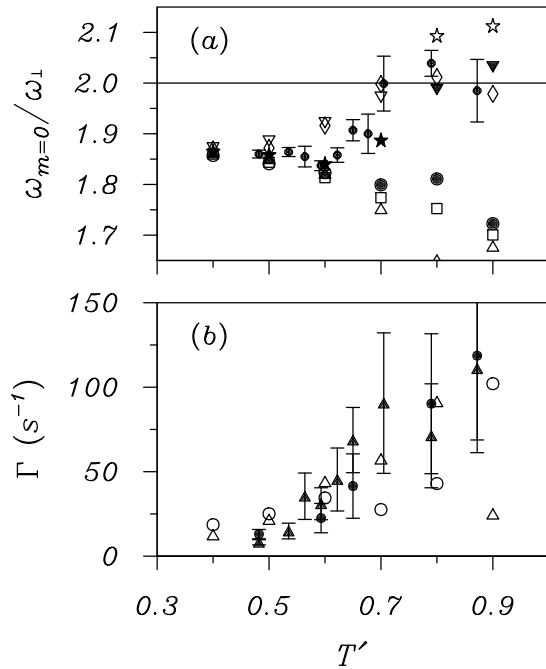


FIG. 3. (a) Frequency of the $m = 0$ mode as a function of temperature, with the experimental results of [3] plotted with error bars. We display simulation results for six drive frequencies, with $\Omega = 1.75\omega_{\perp}$ (circles), $\Omega = 1.80\omega_{\perp}$ (squares), $\Omega = 1.85\omega_{\perp}$ (triangles), $\Omega = 1.90\omega_{\perp}$ (stars), $\Omega = 1.95\omega_{\perp}$ (diamonds), and $\Omega = 2.00\omega_{\perp}$ (inverted triangles). The filled symbols at each T' represent the drives that produce the two largest condensate responses. (b) Damping rate *versus* T' , where our results (open symbols) are compared to experiment (closed symbols), for the $m = 0$ (triangles) and $m = 2$ (circles) modes.

For completeness, we end by comparing our results for the damping rate against experiment. This is perhaps less instructive, since the experimental data contains large error bars. There are also uncertainties in the damping we obtain at the higher temperatures due to sensitivity of the results to both the form of the drive and the timescale of the fit. However, the scatter in the results at low temperatures is much smaller and, as Fig. 3(b) shows, the damping rates obtained in this temperature range are in good agreement with experiment.

In summary, we study quadrupole oscillations of a Bose condensed gas at finite temperatures using simulations based on the ZNG formalism [12]. This allows us to observe the coupled dynamics of the condensed and noncondensed components of the gas, which are particularly important when considering the $m = 0$ mode where the characteristic frequencies of the two compo-

nents are close. Simultaneous excitation of the condensate and thermal cloud by a harmonic modulation of the trap leads to a cross-over between the two frequencies at high temperatures, in accordance with experimental observations. This agreement, taken with previous studies of the scissors mode [13], indicates that a semiclassical Hartree-Fock description is adequate in describing finite-temperature dynamics in the collisionless regime.

We acknowledge use of the HPCVL computing facility at Queen's University, and financial support from NSERC of Canada.

-
- [1] S. Stringari, Phys. Rev. Lett., **77**, 2360 (1996).
 - [2] D. S. Jin *et al.*, **77**, 420 (1996); M. -O. Mewes *et al.*, **77**, 988 (1996).
 - [3] D. S. Jin, M. R. Matthews, J. R. Ensher, C. E. Wieman, and E. A. Cornell, Phys. Rev. Lett. **78**, 764 (1997).
 - [4] P. O. Fedichev, G. V. Shlyapnikov, and J. T. M. Walraven, Phys. Rev. Lett. **80**, 2269 (1998).
 - [5] J. Reidl, A. Csordás, R. Graham, and P. Szépfalussy, Phys. Rev. A **61**, 043606 (2000).
 - [6] D. A. W. Hutchinson, R. J. Dodd, and K. Burnett, Phys. Rev. Lett. **81**, 2198 (1998).
 - [7] R. A. Duine and H. T. C. Stoof, Phys. Rev. A **65**, 013603 (2002).
 - [8] S. A. Morgan, J. Phys. B **33**, 3847 (2000); M. Rusch, S. A. Morgan, D. A. W. Hutchinson, and K. Burnett, Phys. Rev. Lett. **85**, 4844 (2000).
 - [9] S. Giorgini, Phys. Rev. A **61**, 063615 (2000).
 - [10] M. J. Bijlsma and H. T. C. Stoof, Phys. Rev. A **60**, 3973 (1999).
 - [11] U. Al Khawaja and H. T. C. Stoof, Phys. Rev. A **62**, 053602 (2000).
 - [12] E. Zaremba, T. Nikuni, and A. Griffin, J. Low Temp. Phys. **116**, 277 (1999).
 - [13] B. Jackson and E. Zaremba, Phys. Rev. Lett. **87**, 100404 (2001).
 - [14] O. M. Maragò, G. Hechenblaikner, E. Hodby, and C. J. Foot, Phys. Rev. Lett. **86**, 3938 (2001).
 - [15] B. Jackson and E. Zaremba, preprint cond-mat/0106652.
 - [16] The semiclassical approximation is valid when $k_B T \gg \hbar \bar{\omega}$ (where $\bar{\omega}$ is the geometric mean of the trap frequency), which is well satisfied for the parameters considered here. In a homogeneous condensate the HF approximation is applicable when $k_B T \gg g n_c$, which here corresponds to only higher temperatures. However, the density of excitations in a trapped gas extends the validity of the HF approximation to even lower temperatures [F. Dalfovo *et al.*, Phys. Rev. A **56**, 3840 (1997)].
 - [17] B. Jackson and C. S. Adams, Phys. Rev. A **63**, 053606 (2001).
 - [18] E. A. Cornell, private communication.